

Search for supersymmetry with R-parity violating decays via λ couplings at $\sqrt{s} = 183$ GeV

DELPHI Collaboration

OPEN-99-449
10/12/1998



Search for supersymmetry with R-parity violating decays via λ couplings at $\sqrt{s} = 183$ GeV

DELPHI Collaboration

Abstract

Searches for pair production of supersymmetric particles in e^+e^- collisions at center of mass energy of 183 GeV have been performed on DELPHI data under the assumption that R -parity is not conserved and that only one R -parity violating coupling of λ type is dominant. Since in these models any particle can be the lightest supersymmetric particle, the searches for charginos, neutralinos, sleptons and squarks have been performed both for direct R -parity violating decays and for indirect cascade decays, assuming that the strength of the λ couplings is such that the lifetimes can be neglected. The pair production of supersymmetric particles is used to constrain domains of the parameter space, previously explored under the assumption of R -parity conservation.

P.Abreu²¹, W.Adam⁵⁰, T.Adye³⁶, P.Adzic¹¹, I.Ajinenko⁴², Z.Albrecht¹⁷, T.Alderweireld², G.D.Alekseev¹⁶, R.Aleman⁴⁹, T.Allmendinger¹⁷, P.P.Allport²², S.Almehed²⁴, U.Amaldi⁹, S.Amato⁴⁷, E.G.Anassontzis³, P.Andersson⁴⁴, A.Andreazza⁹, S.Andringa²¹, P.Antilogus²⁵, W-D.Apel¹⁷, Y.Arnaud¹⁴, B.Åsman⁴⁴, J-E.Augustin²⁵, A.Augustinus⁹, P.Bailion⁹, P.Bambade¹⁹, F.Barao²¹, G.Barbiellini⁴⁶, R.Barbier²⁵, D.Y.Bardin¹⁶, G.Barker⁹, A.Baroncelli³⁸, M.Battaglia¹⁵, M.Baubillier²³, K-H.Becks⁵², M.Begalli⁶, P.Beilliere⁸, Yu.Belokopytov^{9,53}, A.C.Benvenuti⁵, C.Berat¹⁴, M.Berggren²⁵, D.Bertini²⁵, D.Bertrand², M.Besancon³⁹, F.Bianchi⁴⁵, M.Biggi⁴⁵, M.S.Bilenky¹⁶, M-A.Bizouard¹⁹, D.Bloch¹⁰, H.M.Blom³⁰, M.Bonesini²⁷, W.Bonivento²⁷, M.Boonekamp³⁹, P.S.L.Booth²², A.W.Borgland⁴, G.Borisov¹⁹, C.Bosio⁴¹, O.Botner⁴⁸, E.Boudinov³⁰, B.Bouquet¹⁹, C.Bourdarios¹⁹, T.J.V.Bowcock²², I.Boyko¹⁶, I.Bozovic¹¹, M.Bozzo¹³, P.Branchini³⁸, T.Brenke⁵², R.A.Brenner⁴⁸, P.Bruckman¹⁸, J-M.Brunet⁸, L.Bugge³², T.Buran³², T.Burgsmueller⁵², P.Buschmann⁵², S.Cabrera⁴⁹, M.Caccia²⁷, M.Calvi²⁷, A.J.Camacho Rozas⁴⁰, T.Camporesi⁹, V.Canale³⁷, F.Carena⁹, L.Carroll²², C.Caso¹³, M.V.Castillo Gimenez⁴⁹, A.Cattai⁹, F.R.Cavallo⁵, V.Chabaud⁹, Ph.Charpentier⁹, L.Chaussard²⁵, P.Checchia³⁵, G.A.Chelkov¹⁶, R.Chierici⁴⁵, P.Chliapnikov⁴², P.Chochula⁷, V.Chorowicz²⁵, J.Chudoba²⁹, P.Collins⁹, R.Contri¹³, E.Cortina⁴⁹, G.Cosme¹⁹, F.Cossutti³⁹, J-H.Cowell²², H.B.Crawley¹, D.Crennell³⁶, S.Crepe¹⁴, G.Crosetti¹³, J.Cuevas Maestro³³, S.Czellar¹⁵, G.Damgaard²⁸, M.Davenport⁹, W.Da Silva²³, A.Deghorain², G.Della Ricca⁴⁶, P.Delpierre²⁶, N.Demaria⁹, A.De Angelis⁹, W.De Boer¹⁷, S.De Brabandere², C.De Clercq², B.De Lotto⁴⁶, A.De Min³⁵, L.De Paula⁴⁷, H.Dijkstra⁹, L.Di Ciaccio³⁷, J.Dolbeau⁸, K.Doroba⁵¹, M.Dracos¹⁰, J.Drees⁵², M.Dris³¹, A.Duperrin²⁵, J-D.Durand^{25,9}, G.Eigen⁴, T.Ekelof⁴⁸, G.Ekspong⁴⁴, M.Ellert⁴⁸, M.Elsing⁹, J-P.Engel¹⁰, B.Erzen⁴³, M.Espirito Santo²¹, E.Falk²⁴, G.Fanourakis¹¹, D.Fassouliotis¹¹, J.Fayot²³, M.Feindt¹⁷, P.Ferrari²⁷, A.Ferrer⁴⁹, E.Ferrer-Ribas¹⁹, S.Fichet²³, A.Firestone¹, U.Flagmeyer⁵², H.Foeth⁹, E.Fokitis³¹, F.Fontanelli¹³, B.Franek³⁶, A.G.Frodesen⁴, R.Fruhworth⁵⁰, F.Fulda-Quenzer¹⁹, J.Fuster⁴⁹, A.Galloni²², D.Gamba⁴⁵, S.Gamblin¹⁹, M.Gandelman⁴⁷, C.Garcia⁴⁹, J.Garcia⁴⁰, C.Gaspar⁹, M.Gaspar⁴⁷, U.Gasparini³⁵, Ph.Gavillet⁹, E.N.Gazis³¹, D.Gele¹⁰, L.Gerdyukov⁴², N.Ghodbane²⁵, I.Gil⁴⁹, F.Glege⁵², R.Gokieli⁵¹, B.Golob⁴³, G.Gomez-Ceballos⁴⁰, P.Goncalves²¹, I.Gonzalez Caballero⁴⁰, G.Gopal³⁶, L.Gorn^{1,54}, M.Gorski⁵¹, Yu.Gouz⁴², V.Gracco¹³, J.Grahl¹, E.Graziani³⁸, C.Green²², H-J.Grimm¹⁷, P.Gris³⁹, G.Grosdidier¹⁹, K.Grzelak⁵¹, M.Gunther⁴⁸, J.Guy³⁶, F.Hahn⁹, S.Hahn⁵², S.Haider⁹, A.Hallgren⁴⁸, K.Hamacher⁵², J.Hansen³², F.J.Harris³⁴, V.Hedberg²⁴, S.Heising¹⁷, J.J.Hernandez⁴⁹, P.Herquet², H.Herr⁹, T.L.Hessing³⁴, J.-M.Heuser⁵², E.Higon⁴⁹, S-O.Holmgren⁴⁴, P.J.Holt³⁴, S.Hoorelbeke², M.Houlden²², J.Hrubic⁵⁰, K.Huet², G.J.Hughes²², K.Hultqvist⁴⁴, J.N.Jackson²², R.Jacobsson⁹, P.Jalocha⁹, R.Janik⁷, Ch.Jarlskog²⁴, G.Jarlskog²⁴, P.Jarry³⁹, B.Jean-Marie¹⁹, E.K.Johansson⁴⁴, P.Jonsson²⁵, C.Joram⁹, P.Juillot¹⁰, F.Kapusta²³, K.Karafasoulis¹¹, S.Katsanevas²⁵, E.C.Katsoufis³¹, R.Keranen¹⁷, B.P.Kersevan⁴³, B.A.Khomenko¹⁶, N.N.Khovanski¹⁶, A.Kiiskinen¹⁵, B.King²², A.Kinvig²², N.J.Kjaer³⁰, O.Klapp⁵², H.Klein⁹, P.Kluit³⁰, P.Kokkinias¹¹, M.Koratzinos⁹, V.Kostioukhine⁴², C.Kourkoumelis³, O.Kouznetsov¹⁶, M.Krammer⁵⁰, C.Kreuter⁹, E.Kriznic⁴³, P.Krstic¹¹, Z.Krumstein¹⁶, P.Kubinec⁷, W.Kucewicz¹⁸, J.Kurowska⁵¹, K.Kurvinen¹⁵, J.W.Lamsa¹, D.W.Lane¹, P.Langefeld⁵², V.Lapin⁴², J-P.Laugier³⁹, R.Lauhakangas¹⁵, G.Leder⁵⁰, F.Ledroit¹⁴, V.Lefebure², L.Leinonen⁴⁴, A.Leisos¹¹, R.Leitner²⁹, G.Lenzen⁵², V.Lepeltier¹⁹, T.Lesiak¹⁸, M.Lethuillier³⁹, J.Libby³⁴, D.Liko⁹, A.Lipniacka⁴⁴, I.Lippi³⁵, B.Loerstad²⁴, J.G.Loken³⁴, J.H.Lopes⁴⁷, J.M.Lopez⁴⁰, R.Lopez-Fernandez¹⁴, D.Loukas¹¹, P.Lutz³⁹, L.Lyons³⁴, J.R.Mahon⁶, A.Maio²¹, A.Malek⁵², T.G.M.Malmgren⁴⁴, V.Malychev¹⁶, F.Mandl⁵⁰, J.Marco⁴⁰, R.Marco⁴⁰, B.Marechal⁴⁷, M.Margoni³⁵, J-C.Marin⁹, C.Mariotti⁹, A.Markou¹¹, C.Martinez-Rivero¹⁹, F.Martinez-Vidal⁴⁹, S.Marti i Garcia⁹, J.Masik¹², N.Mastroiannopoulos¹¹, F.Matorras⁴⁰, C.Matteuzzi²⁷, G.Matthiae³⁷, F.Mazzucato³⁵, M.Mazzucato³⁵, M.Mc Cubbin²², R.Mc Kay¹, R.Mc Nulty²², G.Mc Pherson²², C.Meroni²⁷, W.T.Meyer¹, A.Miagkov⁴², E.Migliore⁴⁵, L.Mirabito²⁵, W.A.Mitaroff⁵⁰, U.Mjoernmark²⁴, T.Moa⁴⁴, M.Moch¹⁷, R.Moeller²⁸, K.Moenig⁹, M.R.Monge¹³, X.Moreau²³, P.Moretini¹³, G.Morton³⁴, U.Mueller⁵², K.Muenich⁵², M.Mulders³⁰, C.Mulet-Marquis¹⁴, R.Muresan²⁴, W.J.Murray³⁶, B.Muryn^{14,18}, G.Myatt³⁴, T.Myklebust³², F.Naraghi¹⁴, F.L.Navarria⁵, S.Navas⁴⁹, K.Nawrocki⁵¹, P.Negri²⁷, S.Nemecek¹², N.Neufeld⁹, N.Neumeister⁵⁰, R.Nicolaidou¹⁴, B.S.Nielsen²⁸, M.Nikolenko^{10,16}, V.Nomokonov¹⁵, A.Normand²², A.Nygren²⁴, V.Obraztsov⁴², A.G.Olshevski¹⁶, A.Onofre²¹, R.Orava¹⁵, G.Orazi¹⁰, K.Osterberg¹⁵, A.Ouraou³⁹, M.Paganoni²⁷, S.Paiano⁵, R.Pain²³, R.Paiva²¹, J.Palacios³⁴, H.Palka¹⁸, Th.D.Papadopoulou³¹, K.Papageorgiou¹¹, L.Pape⁹, C.Parkes³⁴, F.Parodi¹³, U.Parzefall²², A.Passeri³⁸, O.Passon⁵², M.Pegoraro³⁵, L.Peralta²¹, M.Pernicka⁵⁰, A.Perrotta⁵, C.Petridou⁴⁶, A.Petrolini¹³, H.T.Phillips³⁶, F.Pierre³⁹, M.Pimenta²¹, E.Piotto²⁷, T.Podobnik⁴³, M.E.Pol⁶, G.Polok¹⁸, P.Poropat⁴⁶, V.Pozdniakov¹⁶, P.Privitera³⁷, N.Pukhaeva¹⁶, A.Pullia²⁷, D.Radojicic³⁴, S.Ragazzi²⁷, H.Rahmani³¹, D.Rakoczy⁵⁰, P.N.Ratoff²⁰, A.L.Read³², P.Rebecchi⁹, N.G.Redaeli²⁷, M.Regler⁵⁰, D.Reid³⁰, R.Reinhardt⁵², P.B.Renton³⁴, L.K.Resvanis³, F.Richard¹⁹, J.Ridky¹², G.Rinaudo⁴⁵, O.Rohne³², A.Romero⁴⁵, P.Ronchese³⁵, E.I.Rosenberg¹, P.Rosinsky⁷, P.Roudeau¹⁹, T.Rovelli⁵, Ch.Royon³⁹, V.Ruhlmann-Kleider³⁹, A.Ruiz⁴⁰, H.Saarikko¹⁵, Y.Sacquin³⁹, A.Sadovsky¹⁶, G.Sajot¹⁴, J.Salt⁴⁹, D.Sampsonidis¹¹, M.Sannino¹³, H.Schneider¹⁷, Ph.Schwemling²³, U.Schwickerath¹⁷, M.A.E.Schyns⁵², F.Scuri⁴⁶, P.Seager²⁰, Y.Sedykh¹⁶, A.M.Segar³⁴, R.Sekulin³⁶, R.C.Shellard⁶, A.Sheridan²², M.Siebel⁵², L.Simard³⁹, F.Simonetto³⁵, A.N.Sisakian¹⁶, G.Smadja²⁵, N.Smirnov⁴², O.Smirnova²⁴, G.R.Smith³⁶, O.Solovianov⁴², A.Sopczak¹⁷, R.Sosnowski⁵¹, T.Spaso²¹, E.Spiriti³⁸, P.Sponholz⁵², S.Squarcia¹³, D.Stampfer⁵⁰, C.Stanescu³⁸, S.Stanic⁴³, K.Stevenson³⁴, A.Stocchi¹⁹, J.Strauss⁵⁰, R.Strub¹⁰, B.Stugu⁴, M.Szczekowski⁵¹, M.Szeptycka⁵¹, T.Tabarelli²⁷, F.Tegenfeldt⁴⁸, F.Terranova²⁷, J.Thomas³⁴, J.Timmermans³⁰, N.Tinti⁵, L.G.Tkatchev¹⁶, S.Todorova¹⁰, D.Z.Toet³⁰, A.Tomaradze², B.Tome²¹, A.Tonazzo²⁷, L.Tortora³⁸, G.Transtromer²⁴, D.Treille⁹, G.Tristram⁸

M.Trochimczuk⁵¹, C.Troncon²⁷, A.Tsirou⁹, M-L.Turluer³⁹, I.A.Tyapkina¹⁶, S.Tzamarias¹¹, B.Ueberschaer⁵², O.Ullaland⁹, V.Uvarov⁴², G.Valenti⁵, E.Vallazza⁴⁶, G.W.Van Apeldoorn³⁰, P.Van Dam³⁰, J.Van Eldik³⁰, A.Van Lysebetten², I.Van Vulpen³⁰, N.Vassilopoulos³⁴, G.Vegni²⁷, L.Ventura³⁵, W.Venus^{9,36}, F.Verbeure², M.Verlato³⁵, L.S.Vertogradov¹⁶, V.Verzi³⁷, D.Vilanova³⁹, L.Vitale⁴⁶, E.Vlasov⁴², A.S.Vodopyanov¹⁶, C.Vollmer¹⁷, G.Voulgaris³, V.Vrba¹², H.Wahlen⁵², C.Walck⁴⁴, C.Weiser¹⁷, D.Wicke⁵², J.H.Wickens², G.R.Wilkinson⁹, M.Winter¹⁰, M.Witek¹⁸, G.Wolf⁹, J.Yi¹, O.Yushchenko⁴², A.Zalewska¹⁸, P.Zalewski⁵¹, D.Zavrtanik⁴³, E.Zevgolatakos¹¹, N.I.Zimin^{16,24}, G.C.Zucchelli⁴⁴, G.Zumerle³⁵

¹Department of Physics and Astronomy, Iowa State University, Ames IA 50011-3160, USA

²Physics Department, Univ. Instelling Antwerpen, Universiteitsplein 1, BE-2610 Wilrijk, Belgium and IIHE, ULB-VUB, Pleinlaan 2, BE-1050 Brussels, Belgium

and Faculté des Sciences, Univ. de l'Etat Mons, Av. Maistriau 19, BE-7000 Mons, Belgium

³Physics Laboratory, University of Athens, Solonos Str. 104, GR-10680 Athens, Greece

⁴Department of Physics, University of Bergen, Allégaten 55, NO-5007 Bergen, Norway

⁵Dipartimento di Fisica, Università di Bologna and INFN, Via Irnerio 46, IT-40126 Bologna, Italy

⁶Centro Brasileiro de Pesquisas Físicas, rua Xavier Sigaud 150, BR-22290 Rio de Janeiro, Brazil and Depto. de Física, Pont. Univ. Católica, C.P. 38071 BR-22453 Rio de Janeiro, Brazil

and Inst. de Física, Univ. Estadual do Rio de Janeiro, rua São Francisco Xavier 524, Rio de Janeiro, Brazil

⁷Comenius University, Faculty of Mathematics and Physics, Mlynska Dolina, SK-84215 Bratislava, Slovakia

⁸Collège de France, Lab. de Physique Corpusculaire, IN2P3-CNRS, FR-75231 Paris Cedex 05, France

⁹CERN, CH-1211 Geneva 23, Switzerland

¹⁰Institut de Recherches Subatomiques, IN2P3 - CNRS/ULP - BP20, FR-67037 Strasbourg Cedex, France

¹¹Institute of Nuclear Physics, N.C.S.R. Demokritos, P.O. Box 60228, GR-15310 Athens, Greece

¹²FZU, Inst. of Phys. of the C.A.S. High Energy Physics Division, Na Slovance 2, CZ-180 40, Praha 8, Czech Republic

¹³Dipartimento di Fisica, Università di Genova and INFN, Via Dodecaneso 33, IT-16146 Genova, Italy

¹⁴Institut des Sciences Nucléaires, IN2P3-CNRS, Université de Grenoble 1, FR-38026 Grenoble Cedex, France

¹⁵Helsinki Institute of Physics, HIP, P.O. Box 9, FI-00014 Helsinki, Finland

¹⁶Joint Institute for Nuclear Research, Dubna, Head Post Office, P.O. Box 79, RU-101 000 Moscow, Russian Federation

¹⁷Institut für Experimentelle Kernphysik, Universität Karlsruhe, Postfach 6980, DE-76128 Karlsruhe, Germany

¹⁸Institute of Nuclear Physics and University of Mining and Metallurgy, Ul. Kawiorów 26a, PL-30055 Krakow, Poland

¹⁹Université de Paris-Sud, Lab. de l'Accélérateur Linéaire, IN2P3-CNRS, Bât. 200, FR-91405 Orsay Cedex, France

²⁰School of Physics and Chemistry, University of Lancaster, Lancaster LA1 4YB, UK

²¹LIP, IST, FCUL - Av. Elias Garcia, 14-1º, PT-1000 Lisboa Codex, Portugal

²²Department of Physics, University of Liverpool, P.O. Box 147, Liverpool L69 3BX, UK

²³LPNHE, IN2P3-CNRS, Univ. Paris VI et VII, Tour 33 (RdC), 4 place Jussieu, FR-75252 Paris Cedex 05, France

²⁴Department of Physics, University of Lund, Sölvegatan 14, SE-223 63 Lund, Sweden

²⁵Université Claude Bernard de Lyon, IPNL, IN2P3-CNRS, FR-69622 Villeurbanne Cedex, France

²⁶Univ. d'Aix - Marseille II - CPP, IN2P3-CNRS, FR-13288 Marseille Cedex 09, France

²⁷Dipartimento di Fisica, Università di Milano and INFN, Via Celoria 16, IT-20133 Milan, Italy

²⁸Niels Bohr Institute, Blegdamsvej 17, DK-2100 Copenhagen Ø, Denmark

²⁹NC, Nuclear Centre of MFF, Charles University, Areal MFF, V Holesovickach 2, CZ-180 00, Praha 8, Czech Republic

³⁰NIKHEF, Postbus 41882, NL-1009 DB Amsterdam, The Netherlands

³¹National Technical University, Physics Department, Zografou Campus, GR-15773 Athens, Greece

³²Physics Department, University of Oslo, Blindern, NO-1000 Oslo 3, Norway

³³Dpto. Física, Univ. Oviedo, Avda. Calvo Sotelo s/n, ES-33007 Oviedo, Spain

³⁴Department of Physics, University of Oxford, Keble Road, Oxford OX1 3RH, UK

³⁵Dipartimento di Fisica, Università di Padova and INFN, Via Marzolo 8, IT-35131 Padua, Italy

³⁶Rutherford Appleton Laboratory, Chilton, Didcot OX11 0QX, UK

³⁷Dipartimento di Fisica, Università di Roma II and INFN, Tor Vergata, IT-00173 Rome, Italy

³⁸Dipartimento di Fisica, Università di Roma III and INFN, Via della Vasca Navale 84, IT-00146 Rome, Italy

³⁹DAPNIA/Service de Physique des Particules, CEA-Saclay, FR-91191 Gif-sur-Yvette Cedex, France

⁴⁰Instituto de Física de Cantabria (CSIC-UC), Avda. los Castros s/n, ES-39006 Santander, Spain

⁴¹Dipartimento di Fisica, Università degli Studi di Roma La Sapienza, Piazzale Aldo Moro 2, IT-00185 Rome, Italy

⁴²Inst. for High Energy Physics, Serpukov P.O. Box 35, Protvino, (Moscow Region), Russian Federation

⁴³J. Stefan Institute, Jamova 39, SI-1000 Ljubljana, Slovenia and Laboratory for Astroparticle Physics,

Nova Gorica Polytechnic, Kostanjevska 16a, SI-5000 Nova Gorica, Slovenia,

and Department of Physics, University of Ljubljana, SI-1000 Ljubljana, Slovenia

⁴⁴Fysikum, Stockholm University, Box 6730, SE-113 85 Stockholm, Sweden

⁴⁵Dipartimento di Fisica Sperimentale, Università di Torino and INFN, Via P. Giuria 1, IT-10125 Turin, Italy

⁴⁶Dipartimento di Fisica, Università di Trieste and INFN, Via A. Valerio 2, IT-34127 Trieste, Italy

and Istituto di Fisica, Università di Udine, IT-33100 Udine, Italy

⁴⁷Univ. Federal do Rio de Janeiro, C.P. 68528 Cidade Univ., Ilha do Fundão BR-21945-970 Rio de Janeiro, Brazil

⁴⁸Department of Radiation Sciences, University of Uppsala, P.O. Box 535, SE-751 21 Uppsala, Sweden

⁴⁹IFIC, Valencia-CSIC, and D.F.A.M.N., U. de Valencia, Avda. Dr. Moliner 50, ES-46100 Burjassot (Valencia), Spain

⁵⁰Institut für Hochenergiephysik, Österr. Akad. d. Wissensch., Nikolsdorfergasse 18, AT-1050 Vienna, Austria

⁵¹Inst. Nuclear Studies and University of Warsaw, Ul. Hoza 69, PL-00681 Warsaw, Poland

⁵²Fachbereich Physik, University of Wuppertal, Postfach 100 127, DE-42097 Wuppertal, Germany

⁵³On leave of absence from IHEP Serpukhov

⁵⁴Now at University of Florida

1 Introduction

This paper presents the searches for pair produced neutralinos, charginos and sfermions in the hypothesis of R -parity violation with only one dominant λ_{ijk} coupling, performed in the data sample collected by the DELPHI detector at center-of-mass energy of 183 GeV.

1.1 The R -parity violating Lagrangian

In the Minimal Supersymmetric extension of the Standard Model (MSSM) [1], the interactions are consistent with a $B - L$ conservation ($B =$ baryon number, $L =$ lepton number). As a consequence, the MSSM possesses a multiplicative R -parity invariance, where $R = (-1)^{3B+L+2S}$ for a particle with spin S [2]. Standard particles have even R -parity, and the corresponding superpartners have odd R -parity.

One approach to go *beyond the MSSM* is to retain the minimal particle content of the MSSM, but remove the assumption of R -parity invariance. In this scenario, new interactions violating B or L conservation appear, which can be introduced in the superpotential as [3]:

$$\lambda_{ijk} L_i L_j \bar{E}_k + \lambda'_{ijk} L_i Q_j \bar{D}_k + \lambda''_{ijk} \bar{U}_i \bar{D}_j \bar{D}_k$$

where i, j and k are the generation indices; L and E denote the lepton superfields and Q, U, D the quark superfields; $\lambda_{ijk}, \lambda'_{ijk}$ and λ''_{ijk} are the new Yukawa couplings. The two first terms violate L conservation, and the third one B conservation. Since $\lambda_{ijk} = -\lambda_{jik}, \lambda''_{ijk} = -\lambda''_{ikj}$, there are 9 $\lambda_{ijk}, 27 \lambda'_{ijk}$ and 9 λ''_{ijk} leading to 45 new couplings. Nevertheless, all R -parity violating (\mathcal{R}_p) terms cannot be simultaneously present, otherwise the proton would rapidly decay [4,?].

One major phenomenological consequence of \mathcal{R}_p is that the Lightest Supersymmetric Particle (LSP) is allowed to decay to standard fermions. This fact modifies the signatures of the supersymmetric particle production compared to the expected signatures in case of R -parity conservation. Moreover, single sparticle production is possible [6].

1.2 Pair production of neutralinos, charginos and sfermions

In the MSSM, the masses and mixing angles of the neutralinos and the charginos are determined by the values of the four parameters M_1, M_2 , the U(1) and SU(2) gaugino mass parameters at the electroweak scale, μ , the mixing mass term of the Higgs doublets at the electroweak scale and $\tan\beta$, the ratio of the vacuum expectation values of the two Higgs doublets. The assumption that the gaugino masses are unified at the GUT scale, implies $M_1 = \frac{5}{3}\tan^2\theta_W M_2 \simeq \frac{1}{2}M_2$ at the electroweak scale.

The neutralinos and charginos are pair-produced in the s -channel via a γ or a Z , or via a t -channel exchange of a selectron (sneutrino) for the neutralinos (charginos), if the slepton masses are low enough (Fig. 1). It is also assumed that m_0 , the scalar common mass at the GUT scale, determines the slepton masses. When the selectron mass is sufficiently small ($\ll 100$ GeV/ c^2), the neutralino production can be enhanced, because of the t -channel \tilde{e} exchange contribution. On the contrary, if the $\tilde{\nu}_e$ mass is in the same range, the chargino cross section can decrease due to destructive interference between the s - and t -channel amplitudes. If the dominant component of neutralinos and charginos is the higgsino ($|\mu| \ll M_2$), the production cross sections are large and insensitive to slepton masses. The appropriate MSSM parameters to consider in the general scan are then M_2 ,

μ , $\tan\beta$ and m_0 . Depending on the values of the different parameters, the cross sections at $\sqrt{s} = 183$ GeV vary typically from 0.1 to 10 pb.

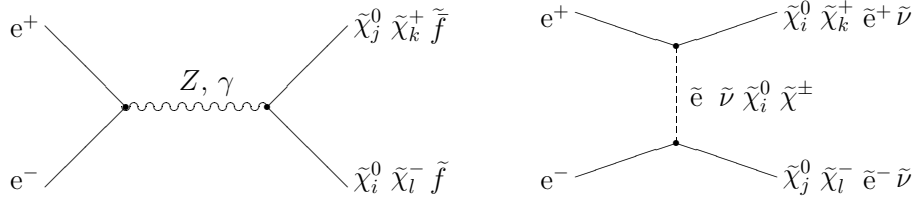


Figure 1: Neutralino, chargino and sfermion pair production diagrams ($i, j = 1, \dots, 4$; $k, l = 1, 2$). In the s -channel neutralinos and neutral sfermions are produced only via the Z .

The sfermions can be produced via the exchange in the s -channel of a Z (and (or) a γ for the charged) (Fig. 1); the production cross section is function of the sfermion mass. In the case of the third generation the mixing angle also enters in the production cross section. The $\tilde{\nu}_e$ (\tilde{e}) can also be produced via the exchange of a chargino (neutralino) in the t -channel, and then the cross section depends also on the $\tilde{\chi}^\pm$ ($\tilde{\chi}^0$) mass and through them to the four MSSM parameters mentioned above.

1.3 Direct and indirect decays of neutralinos, charginos and sfermions

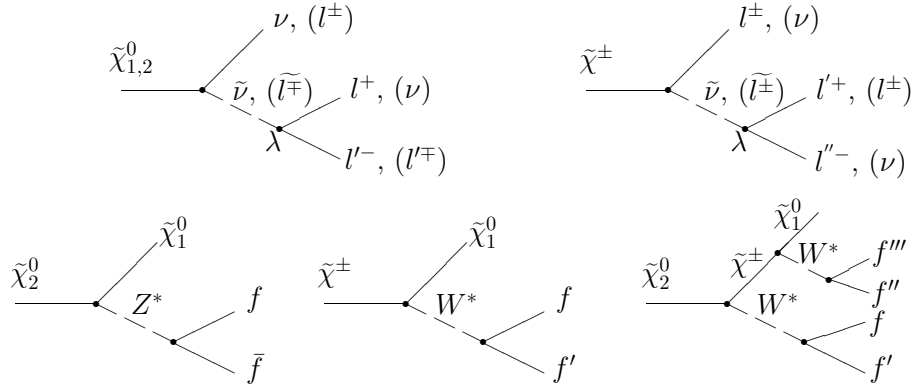


Figure 2: Upper part: $\tilde{\chi}^0$ and $\tilde{\chi}^\pm$ direct decay; in these diagrams the λ indicates the R_p vertex. lower part: $\tilde{\chi}^0$ and $\tilde{\chi}^\pm$ indirect decay; the subsequent neutralino R_p decay is shown in the upper part.

The decay can be either direct or indirect. In a *direct decay* the sparticle decays directly or via a sparticle virtual exchange to standard particles through an R_p vertex. This is always the case when the sparticle is the LSP. If for example the $\tilde{\nu}$ is the LSP, it can decay directly into a pair of charged leptons through the λ_{ijk} R_p operators. If on the other hand the lightest neutralino $\tilde{\chi}_1^0$ is the LSP, then it can decay into a lepton and virtual slepton pair with the subsequent decay of the slepton to leptons via the R -parity violating λ couplings (see Fig. 2).

In an *indirect decay* the sparticle first decays through an R_p -conserving vertex to a standard and on-shell particle which then decays through an R_p vertex. This mode

usually dominates when there is enough phase space between “mother” and “daughter” sparticles. As a rule of thumb, when the difference of masses between these two sparticles is larger than 5–10 GeV the indirect mode tends to dominate. But regions of the parameter space where one has a “dynamic” suppression of the R_p conserving modes also exist. In this case, even if the sparticle is not the LSP, it decays through an R_p mode. A typical example of indirect decay is the R_p decay $\tilde{\chi}_1^+ \rightarrow \tilde{\chi}_1^0 + W^{*+}$ and the subsequent decay of $\tilde{\chi}_1^0$ through the R_p couplings (see Fig. 2).

In the case of a dominant λ_{ijk} coupling, the sleptons couple to the leptons. The decay of the lightest neutralino leads to one neutrino and two charged leptons. The heavier neutralinos and the charginos, depending on their mass difference with $\tilde{\chi}_1^0$, can either decay directly into three leptons, or decay to $\tilde{\chi}_1^0$, via for example virtual Z or W, as illustrated on Fig. 2 and in Table 1. Note that, even if the λ couplings lead to purely leptonic decay modes of the lightest neutralino, the indirect decay of chargino or heavier neutralinos may contain some hadronic activity, depending on the decay modes of W^* and Z^* . In order to cover both the direct and indirect decays of $\tilde{\chi}_i^0$ and $\tilde{\chi}^\pm$, the analysis has to be sensitive to the final states listed in Table 2.

Direct decay	$\tilde{\chi}_1^0 \rightarrow \nu l^+ l^-$	$\tilde{\chi}_2^0 \rightarrow \nu l^+ l^-$	$\tilde{\chi}_1^\pm \rightarrow \nu \nu l^\pm, l^+ l^- l^\pm$
Indirect decay		$\tilde{\chi}_2^0 \rightarrow Z^* \tilde{\chi}_1^0, Z^* \rightarrow ff$ $\tilde{\chi}_2^0 \rightarrow \tilde{\chi}_1^0 l^+ l^-, \tilde{\chi}_1^0 \gamma$	$\tilde{\chi}_1^\pm \rightarrow W^{*+} \tilde{\chi}_1^0, W^{*+} \rightarrow ff'$ $\tilde{\chi}_1^\pm \rightarrow \tilde{\chi}_1^0 \nu l^\pm$

Table 1: Possible decays of neutralinos and charginos when a λ coupling is dominant.

Final states	Direct decay of	Indirect decay of
$2l + \cancel{E}$	$\tilde{\chi}_1^+ \tilde{\chi}_1^-$	
$4l + \cancel{E}$	$\tilde{\chi}_1^0 \tilde{\chi}_1^0, \tilde{\chi}_1^+ \tilde{\chi}_1^-$	$\tilde{\chi}_2^0 \tilde{\chi}_1^0$
$6l$	$\tilde{\chi}_1^+ \tilde{\chi}_1^-$	
$6l + \cancel{E}$		$\tilde{\chi}_1^+ \tilde{\chi}_1^-, \tilde{\chi}_2^0 \tilde{\chi}_1^0$
$4l + 2 \text{ jets} + \cancel{E}$		$\tilde{\chi}_2^0 \tilde{\chi}_1^0$
$4l + 4 \text{ jets} + \cancel{E}$		$\tilde{\chi}_1^+ \tilde{\chi}_1^-$
$5l + 2 \text{ jets} + \cancel{E}$		$\tilde{\chi}_1^+ \tilde{\chi}_1^-$

Table 2: Final states in $\tilde{\chi}_i^0, \tilde{\chi}^\pm$ pair production when a λ coupling is dominant ($\cancel{E} \equiv$ missing energy).

The pair production of sneutrinos ($\tilde{\nu}$) and charged sleptons (\tilde{l}) is also studied, since a dominant λ coupling allows them to decay into standard leptons and neutrinos. If the $\tilde{\nu}$ is the LSP, with a mass lower than or very close to that of the $\tilde{\chi}_1^0$ or $\tilde{\chi}^\pm$ mass, it decays directly into two leptons with no missing energy. If it is not the LSP, the indirect decays $\tilde{\nu} \rightarrow \tilde{\chi}_1^0 \nu, \tilde{\nu} \rightarrow \tilde{\chi}_2^0 \nu, \tilde{\nu} \rightarrow \tilde{\chi}^\pm l^\mp$ are allowed, depending on the MSSM parameters; the $\tilde{\chi}_2^0$ and $\tilde{\chi}^\pm$ could also decay directly or indirectly, as previously explained. Furthermore the so called “mixed decay” is possible when from a $\tilde{\nu}$ pair, one $\tilde{\nu}$ decays directly and the second indirectly.

The direct decay of a charged slepton with a λ_{ijk} coupling gives a charged lepton plus a neutrino, while the indirect decay $\tilde{l} \rightarrow \tilde{\chi}_1^0 l$ is dominant in most of the MSSM parameter space. In the latter case, the final state consists of six charged leptons plus missing energy. A mixed decay (one charged slepton decaying directly, the other one indirectly) is also possible. The final states resulting from slepton pair production are listed in Table 3.

Decay type		Pair production signature
Direct	$\tilde{\nu} \rightarrow l^+ l^-$	$4l$
Indirect	$\tilde{\nu} \rightarrow \nu \tilde{\chi}_1^0$	$4l + \cancel{E}$
	$\tilde{\nu} \rightarrow \nu \tilde{\chi}_2^0$	same as $\tilde{\chi}$ analyses
	$\tilde{\nu} \rightarrow l^\pm \tilde{\chi}^\pm$	multilepton or lepton+jets
Direct	$\tilde{l}^\pm \rightarrow l^\pm \nu$	$2l(\text{acoplanar}) + \cancel{E}$ (like R_p signal $\tilde{l}^\pm \rightarrow l^\pm \tilde{\chi}_1^0$ with $M_{\tilde{\chi}^0} = 0$)
Indirect	$\tilde{l}^\pm \rightarrow l^\pm \tilde{\chi}_1^0$	same as $\tilde{\chi}$ analyses
	$\tilde{l}^\pm \rightarrow \nu \tilde{\chi}^\pm$	with ≤ 2 extra leptons or \cancel{E}

Table 3: Final states in charged slepton and sneutrino pair production when a λ coupling is dominant.

Finally, the indirect squark decays into a quark and a neutralino (such as $\tilde{t} \rightarrow c\tilde{\chi}_1^0$), where the neutralino decays via a λ coupling, are also considered in this paper, but only for the stop quark which is supposed to be the lightest squark.

1.4 λ_{ijk} couplings

In case of pair production of supersymmetric particles, R_p is conserved at the production vertex; the cross section does not depend on the R_p couplings. On the contrary, the R_p decay width depends on the λ coupling strength, which then determines the mean decay length of the LSP. If the LSP is a neutralino or a chargino, the mean decay length is given by [7,8]:

$$L(cm) = 0.3 (\beta\gamma) \left(\frac{m_{\tilde{l}}}{100 \text{ GeV}/c^2} \right)^4 \left(\frac{1 \text{ GeV}/c^2}{m_{\tilde{\chi}}} \right)^5 \frac{1}{\lambda^2} \quad (1)$$

where $\lambda = \lambda_{ijk}$ and $\beta\gamma = P_{\tilde{\chi}}/m_{\tilde{\chi}}$. If the LSP is a sfermion, it is given by:

$$L(cm) = 10^{-12} (\beta\gamma) \left(\frac{1 \text{ GeV}/c^2}{m_{\tilde{f}}} \right) \frac{1}{\lambda^2} \quad (2)$$

The condition that the LSP decays close to the production vertex ($L \lesssim 1$ cm) for typical masses considered in this study, implies a lower limit in sensitivity on the λ coupling in the order of 10^{-4} to 10^{-5} in case of $\tilde{\chi}^0$, $\tilde{\chi}^\pm$, and 10^{-7} in case of sfermions. If the LSP is a $\tilde{\chi}$ with low mass and high boost, it can escape detection before decaying. Therefore the assumption of a negligible LSP lifetime restricts the sensitivity of the analysis described in this paper to $M_{\chi_{LSP}}$ greater than $10 \text{ GeV}/c^2$.

Upper limits on the λ_{ijk} couplings can be derived from Standard Model processes [6,?,10], mainly charged-current universality, lepton universality, $\nu_\mu - e$ scattering, forward-backward asymmetry in e^+e^- collisions, and bounds on ν_e -Majorana mass. Most present indirect limits on the λ couplings derived from SM processes are in the range of 10^{-3} to 10^{-1} ; the most stringent upper limit is given for λ_{133} .

For all the analyses presented in this paper, it was assumed that only one λ_{ijk} is dominant. Two kinds of searches have been performed:

- The first assuming that λ_{122} is dominant (i.e the charged leptons coming from \mathcal{R}_p decay are muons and electrons). In this case the neutralino can decay into $e\nu_\mu\mu$ ($\approx 50\%$), or $\mu\nu_e\mu$ ($\approx 50\%$); then the corresponding final state for $\tilde{\chi}_1^0$ pair production is: missing energy, coming from the undetected neutrinos, plus $2e2\mu$ ($\approx 25\%$) or $1e3\mu$ ($\approx 50\%$) or 4μ ($\approx 25\%$). This is the most efficient case since the selection criteria depends on e and μ identification.
- The second assuming that λ_{133} is dominant, meaning that the leptons from \mathcal{R}_p decay are mainly taus, and electrons. This is the least efficient case because of the presence of several taus in the final state.

The efficiencies for the other λ_{ijk} couplings lie between these two extreme cases.

2 Data samples

The data corresponding to an integrated luminosity of 53 pb^{-1} collected during 1997 by the DELPHI detector [11] at center of mass energy around 183 GeV were analysed. For the analyses depending on electron identification, an integrated luminosity of 50.7 pb^{-1} was used in order to remove events affected by problems occurring in the High-density Projection Chamber (HPC).

Concerning the background, the different contributions coming from the Standard Model processes: $e^+e^- \rightarrow Z\gamma$, $\gamma\gamma$, e^+e^- , $W\nu_e$, Ze^+e^- , W^+W^- , ZZ were considered. For the study of four fermion final states, the PYTHIA [12] generator was used; a cross check was performed using the four-fermion final states generated with EXCALIBUR [13]. Two-photon ($\gamma\gamma$) interactions leading to leptonic final states were generated with the BDK program [14]; the $\gamma\gamma \rightarrow$ hadrons were generated using TWOGAM [15]. The $Z\gamma \rightarrow$ hadrons, $\tau^+\tau^-$ and $\mu^+\mu^-$ event samples were produced by PYTHIA, KORALZ [16] and DYMU3 [17] respectively. For processes such as bhabha scattering and two-photon interactions, biased samples were used.

To evaluate signal efficiencies, sparticle production was generated using SUSYGEN [18]. Neutralino and chargino pair productions were considered in several points in the MSSM parameter space, corresponding to different values of $\tan\beta$ (from 1 to 30), m_0 (between $0 \text{ GeV}/c^2$ and $500 \text{ GeV}/c^2$), μ (between minus $200 \text{ GeV}/c^2$ and $200 \text{ GeV}/c^2$) and M_2 (between 0 and $400 \text{ GeV}/c^2$), for both λ couplings considered in the analysis. To study the sneutrino pair production, several signal configurations were generated: a $\tilde{\nu}$ mass range from 50 to $90 \text{ GeV}/c^2$ was covered, with λ_{133} or λ_{122} coupling, and with $\text{Br}(\tilde{\nu} \rightarrow l^+l^-) = 100\%$. Events with sneutrino indirect decay were also simulated, for different $\tilde{\nu}$ and $\tilde{\chi}$ masses, in order to cover several ranges of mass difference between sneutrinos and neutralinos. The same type of procedure was applied to simulate charged slepton pair production and to study their direct and indirect decays. Finally, the stop decays into a charm quark and a neutralino with the subsequent \mathcal{R}_p decay of the neutralino into leptons via a λ_{ijk} coupling were also generated for several sets of stop and neutralino masses.

The λ parameters, when simulating signal events, have been set to their present experimental upper limits: $\lambda_{122} = 0.04$ and $\lambda_{133} = 0.003$.

All generated signal events were processed with the DELPHI detector simulation program.

3 Analyses description

3.1 Neutralinos and charginos decaying through λ

As already mentioned, the indirect decays of neutralinos or charginos can give two or more jets in the final state, beside the leptons and the missing energy. Moreover, in case of the λ_{133} coupling, the τ decays give isolated leptons or thin jets. The DURHAM [19] algorithm is used to reconstruct the jets. In order to cover the different topologies, the jet number is not fixed, and the jet charged multiplicity can be low (thin jets with one track are possible), or can be zero in case of neutral jets. For each event, DURHAM is applied to reconstruct from two to eight jets, and the corresponding jet parameters are stored. The analyses described below are designed to cover all the final states listed in Table 2 as well as final states produced when the chargino is the LSP except the $2l + \cancel{E}$ topology coming from the direct chargino decays, as the region in the MSSM parameter space where this decay dominates is already covered by other studied processes.

3.1.1 λ_{122} case

Events are selected if they satisfy the following criteria:

- the charged multiplicity has to be greater than three as the minimum number of charged tracks expected in these topologies is four;
- the missing p_t is greater than 5 GeV/ c and the polar angle of the missing momentum is between 20 and 160 degrees.

This set of cuts reduces mainly the background coming from bhabha scattering and two-photon processes. The following criteria are based on the lepton characteristics of the signal:

- at least two well identified (standard or tight)[11] muons are required;
- the energy of the most energetic identified lepton must be greater than $10\% \sqrt{s}$;
- an isolation criterion is imposed for the identified leptons (no other charged particle in a half cone of seven degrees around the lepton).

At this stage, most of the hadronic final states of $Z\gamma$, ZZ and W^+W^- processes are removed. The final criteria are designed to reduce the remaining semi-leptonic four fermion final states:

- at least two of the identified leptons must be leading particles in the jets;
- the polar angle of the jets in case of 4, 5, or 6 jet topologies must be between 20 and 160 degrees;
- the missing energy is at least $20\% \sqrt{s}$.

At the end of the selection procedure, no event remains, while 0.7 events are expected from Standard Model processes, most of which come from W^+W^- (as reported at Table 4). For $\tilde{\chi}_1^0 \tilde{\chi}_1^0$ the selection efficiencies are in the range 45–60%, for $\tilde{\chi}_1^+ \tilde{\chi}_1^-$: 20–50%; and for $\tilde{\chi}_2^0 \tilde{\chi}_1^0$: 25–40%, for all the values of μ, M_2 planes considered (see Table 7).

Data	MC	$Z\gamma$	W^+W^-	ZZ
0	0.70 ± 0.14	0.10 ± 0.11	0.40 ± 0.08	0.23 ± 0.03

Table 4: SM background contributions for λ_{122} gaugino analysis.

3.1.2 λ_{133} case

The τ decay gives isolated leptons or thin jets, plus neutrinos. In this case the missing energy is expected to be higher than in the λ_{122} case due to the presence of neutrinos, coming not only from neutralinos or charginos \tilde{R}_p decay, but also from τ decay.

Events are preselected if they satisfy the following criteria:

- at least one (loose) lepton is identified;
- the number of charged tracks must be greater than three;
- the total energy and the energy from charged particles must be greater than $0.18\sqrt{s}$ and $0.16\sqrt{s}$ respectively.

These cuts remove around 99% of two-photon events.

Several criteria are based on the missing quantities:

- the missing p_t is greater than 5 GeV/c;
- the polar angle of the missing momentum is between 27 and 153 degrees;
- the missing energy is at least $0.30\sqrt{s}$.

These cuts are efficient to suppress the background coming from bhabha, two-photon and $Z\gamma$ events.

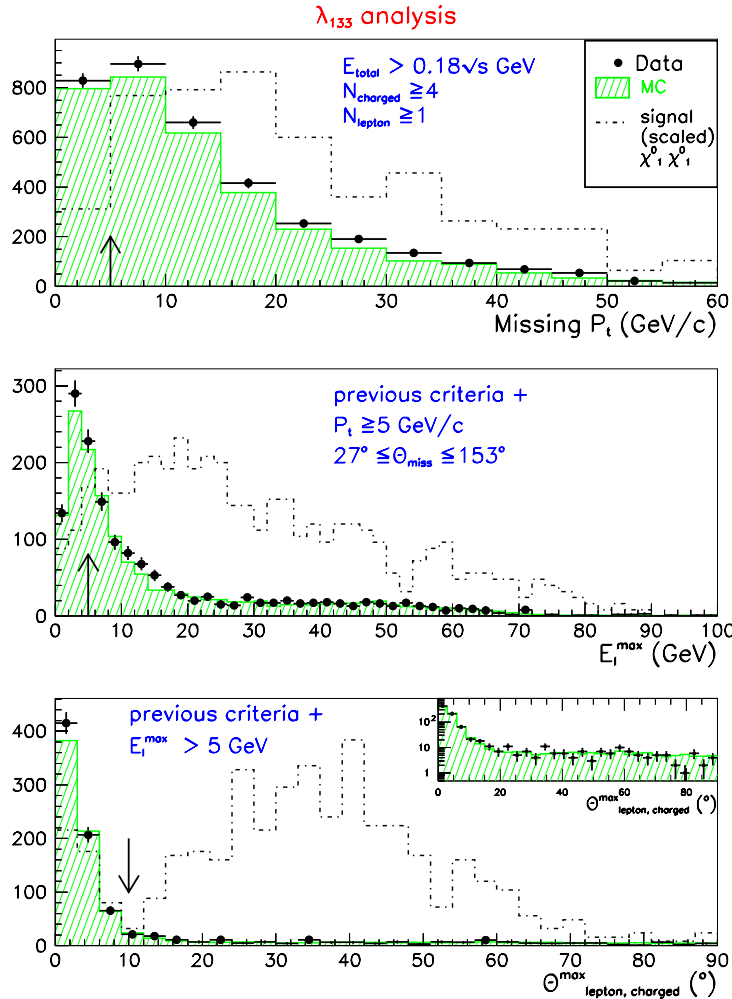


Figure 3: Neutralino and chargino search with the λ_{133} coupling dominant: missing transverse momentum, energy of the most energetic lepton and isolation angle distributions for real data (black dots), expected SM background (hatched) and $\tilde{\chi}_1^0 \tilde{\chi}_1^0$ signal (dotted line). The signal distribution has been scaled (see text). The arrows show the applied cuts.

For the events with fewer than eight charged particles, at least one loose lepton is required, whereas events with eight or more charged particles must have at least two loose leptons. In both cases, the energy of the most energetic lepton must be greater than 5 GeV, and there should be no other charged track in a 10 degree half cone around the identified lepton(s). These last criteria remove $Z\gamma$, and hadronic ZZ and W^+W^- events. In Fig. 3 the distributions of the missing p_t , the energy of the most energetic lepton, and the minimum angle between the lepton and the nearest charged particle are presented. The agreement between real data and simulated background is fairly good. The distribution for simulated signal ($\tilde{\chi}_1^0\tilde{\chi}_1^0$) is also plotted; it is scaled by a factor of ~ 10 .

Selection criteria for λ_{133} coupling	data	MC
At least one loose lepton		
$N_{charged} \geq 4$		
$E_{tot} \geq 18\% \sqrt{s}$, $E_{charged} \geq 16\% \sqrt{s}$		
Missing $p_t > 5$ GeV/c, $27^\circ \leq \Theta_{miss} \leq 153^\circ$	1551	1479 ± 13
$E_{max}^l \geq 5$ GeV	996	965 ± 10
$\Theta_{lepton-track}^{min} \geq 10^\circ$	293	286 ± 4
$E_{miss} > 30\% \sqrt{s}$	174	166 ± 3
If $N_{charged} \geq 8$, $N_{lepton} \geq 2$	70	69.2 ± 2.1
$E_{cone}^{30^\circ} \leq 50\% E_{total}$		
$Y_{34} \geq 0.001$	33	29.5 ± 1.2
In case of four or five jets, at least four charged jets	14	17.9 ± 0.9
Case of four jets:		
$E_{min}^j * \theta_{min}^{j_1, j_2} \geq 0.5$ GeV rad,		
$E_{min}^j * \theta_{min}^{j_1, j_2} \geq 5$ GeV rad if $N_{charged} > 8$		
$20^\circ \leq \theta_{jet} \leq 160^\circ$	3	3.3 ± 0.3

Table 5: List of selection criteria for λ_{133} case.

Data	MC	$Z\gamma$	Ze^+e^-	W^+W^-	ZZ
3	3.3 ± 0.3	0.13 ± 0.11	0.14 ± 0.14	2.73 ± 0.23	0.31 ± 0.06

Table 6: SM background contributions.

The final selection is based on the jet characteristics and topologies. First, the Y_{34} ¹ value must be greater than 10^{-3} , which reduces the $Z\gamma$ contribution (Fig. 4). In case of four or five jet topologies, four charged jets are required. In case of a four jet topology, a cut is applied on the value of $E_{min}^j \times \theta_{min}^{j_a, j_b}$ where E_{min}^j is the energy of the less energetic jet, and $\theta_{min}^{j_a, j_b}$ is the minimum angle between 2 jets. These requirements significantly reduce the $Z\gamma$, $\gamma\gamma$, W^+W^- background. The number of remaining real and simulated data events after these cuts are reported in Table 5.

For $\tilde{\chi}_1^0\tilde{\chi}_1^0$ the selection efficiencies are in the range 22–34 %; for $\tilde{\chi}_1^+\tilde{\chi}_1^-$: 20–37%; and for $\tilde{\chi}_2^0\tilde{\chi}_1^0$: 20–25%, for all the μ , M_2 planes considered. Three events remain after the selection procedure with 3.3 expected from standard background processes. The background is mainly due to W^+W^- events (Table 6).

The results obtained for both λ_{122} and λ_{133} coupling are summarized in Table 7.

¹The Y_{34} is the transition value of the Y_{cut} DURHAM distance in which the event flips from four to three jet configuration.

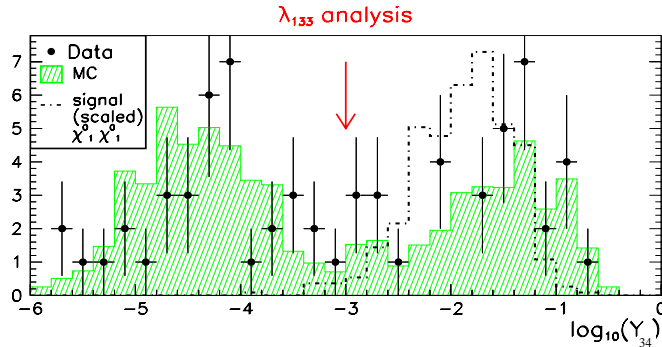


Figure 4: Neutralino and chargino search with a dominant λ coupling: $\log_{10}(Y_{34})$ distribution for real (black dots) and expected SM background (hatched histogram). A scaled signal distribution is also plotted to show that the applied cut removes less than 1% of the signal, and half of the background.

3.2 Sneutrinos decaying through λ

The final state in $\tilde{\nu}\tilde{\nu}$ production is typically purely leptonic. It is the case either for direct decay ($4l$), or for the dominant indirect decay via the lightest neutralino ($4l + \cancel{E}$). The last decay is the indirect dominant mode since the negative chargino search results (see Section 4.1) imply that the indirect decay to $\tilde{\chi}^{\pm}l\bar{\nu}$ is negligible for a $\tilde{\nu}$ with a mass lower than $90 \text{ GeV}/c^2$.

To be more efficient for all these purely leptonic final states, with at least four leptons, the selection criteria have been strengthened with respect to the chargino/neutralino analyses. In case of λ_{122} coupling, the best selection efficiency is obtained from the direct decays as described below; the indirect decays have not been simulated since they lead to final states already covered by the analyses explained before and since the most conservative results are obtained with λ_{133} coupling. In case of λ_{133} coupling, the same analysis is used to study both direct and indirect decays since they lead to the same final state with more or less missing energy.

3.2.1 λ_{122} case

If λ_{122} is the dominant \mathcal{R}_p coupling, the direct decay mode leads to four leptons (μ or/and e) in the final state. The selection criteria are described below:

- the charged multiplicity has to be four;
- at least 2 well identified muons[11] are required;
- the total energy from charged particles has to be greater than $33\%\sqrt{s}$;
- no other charged particle in a half cone of 10 degrees around the lepton, is demanded;
- the total event charge has to be 0;
- the missing energy has to be less than $55\%\sqrt{s}$;
- the thrust value has to be less than 0.95.

No event remains in the data after these cuts with 0.73 expected from standard background processes, mainly from the leptonic final states of the ZZ process (see Table 8). The efficiencies were evaluated by generating sneutrino pair production with masses from 50 to $90 \text{ GeV}/c^2$ and they are in the range of 60–80% depending on the sneutrino mass (Table 10).

3.2.2 λ_{133} case

The preselection criteria are the same as in case of chargino/neutralino studies, except that an upper limit of eight is set on the number of charged tracks, which eliminates more than 90% of all Standard Model backgrounds. A lower cut on the missing energy can be applied even in case of $4l$ final states, due to the τ decay which produces a certain amount of missing energy. But compared to the neutralino decay in which neutrinos are produced directly, the missing energy is less important, therefore the limit is set to $0.1\sqrt{s}$. The missing longitudinal momentum must be lower than $70 \text{ GeV}/c$.

The criteria applied for the identified lepton(s) are also modified. If there are exactly four charged tracks, the minimum angle between a lepton and the nearest charged track must be greater than 20 degrees, otherwise it must be greater than 6 degrees.

As for the chargino/neutralino selection, several criteria are based on the jet characteristics. The DURHAM Y_{34} and Y_{45} values (see Section 3.1.2) must be respectively greater than $1.8 \cdot 10^{-3}$ and $4 \cdot 10^{-4}$. In case of a four jet topology, there must be no neutral jet, at least one jet with its leading track identified as a lepton, and a minimum angle of 20 degrees between 2 jets. The value of $E_{min}^j \times \theta_{min}^{jab}$ (see Section 3.1.2) must be greater than 1 GeV rad, and than 4 GeV rad if $N_{charged} = 8$.

One event remains after this selection with 1.8 expected from standard background processes. The background is mainly due to W^+W^- , $\gamma\gamma$ and ZZ events (Table 9).

In the indirect decay $\tilde{\nu} \rightarrow \nu \tilde{\chi}_1^0$ the final state depends on the λ_{ijk} coupling, since the charged leptons are produced in the $\tilde{\chi}_1^0 \tilde{R}_p$ decay. Therefore the efficiencies do not depend on the sneutrino type, but on the sneutrino and neutralino masses. The selection efficiencies are summarized in Table 10.

3.3 Charged sleptons decaying through λ

For most of the MSSM parameter space studied, the indirect decay of sleptons² in $l\tilde{\chi}_1^0$ is dominant; only in some particular regions, the staus have a non negligible branching fraction into $\nu\tilde{\chi}^\pm$, but this region is excluded by our present limit on the chargino mass (see Section 4.1). The indirect slepton decay gives mostly purely leptonic final state. A particular analysis is devoted to the case of the direct decay of the slepton pair, leading to $2l + \cancel{E}$ final state.

• Analysis concerning the direct slepton decays

With λ_{133} coupling, only the $\tilde{\tau}$ can decay directly, and it has two decay modes: $\tilde{\tau} \rightarrow \tau\nu_e$ (50%), $\tilde{\tau} \rightarrow e\nu_\tau$ (50%). Then the final state in pair production of $\tilde{\tau}$ is: missing energy + ee (25%), $e\tau$ (50%), $\tau\tau$ (25%). Three specific analysis are performed for the three components of the final state. Several preselection criteria are common to the $2e + \cancel{E}$ and $e\tau + \cancel{E}$ analysis:

- the missing p_t must be greater than $20 \text{ GeV}/c$ and the polar angle of the missing momentum must lie between 25 and 155 degrees;
- the acolinearity must be greater than 10 degrees, and the acoplanarity must be less than 160 degrees;
- the energy of the most energetic photon is required to be less than 10 GeV.

Then different criteria are applied to discriminate between the two channels:

$ee + \cancel{E}$ final state

- two loose electrons are required; the angle between them must be at least 10 degrees and at most 160 degrees;

²In this section the term “slepton” means charged slepton

- the energy of each electron has to be greater than 10 GeV, and the sum of their energy less than 110 GeV;
- the neutral multiplicity of the event must be less than 2.

$e\tau + \cancel{E}$ final state

- the charged multiplicity and the neutral multiplicity must both be less than 5;
- at least one loose electron is required, and not more than one identified muon;
- if there is one identified muon, the charged multiplicity must be 2 (one μ , one e);
- the total event charge has to be 0;
- the total energy from charged particles has to be greater than $5\%\sqrt{s}$ and lower than $65\%\sqrt{s}$;
- the minimum angle between the lepton and the closest charged particle must be at least 10 degrees, at most 160 degrees, and the minimum angle between the lepton and the nearest neutral must be greater than 10 degrees;
- the total electromagnetic energy must be at least 10 GeV, and the total leptonic energy must be between 10 and 110 GeV

The results of these 2 analyses are summarized in Table 11.

For the $\tau\tau + \cancel{E}$ final state the analysis performed for the search of R_p conserved $\tilde{\tau} \rightarrow \tau \tilde{\chi}_1^0$ decay [20] has been used: 7 events are selected for 7.5 expected, with an efficiency of 31% which is rather stable in the $\tilde{\tau}$ mass range considered.

• Analysis concerning the indirect slepton decays

In the case of λ_{122} analysis, the most efficient case is studied, namely the indirect smuon decay; the selection criteria consist of:

- charged multiplicity greater than or equal to four,
- at least three well identified muons,
- the total leptonic energy greater than 80 GeV.

In the case of the λ_{133} analysis, the same criteria used for the sneutrino searches are applied. But, contrary to the $\tilde{\nu}$ case, for any given type of coupling, the selection efficiencies depend on the slepton family since in the final state, there is always a lepton of the same flavour. Selection efficiencies depend also on slepton and neutralino masses. Efficiencies and results are reported in Table 12.

3.4 Stop indirect decay

With a λ coupling, only the indirect decay of a squark into a quark and a neutralino (or a chargino) is possible. In the case of stop pair production, each of the stops decays into a charm quark and a neutralino, giving two jets + four charged leptons + missing energy in the final state. This signature is similar to the one produced by the indirect decay of the heavier neutralino into $\tilde{\chi}_1^0$ and Z^* , with one of the Z giving two jets, and the other giving two neutrinos. Therefore the analysis devoted to neutralino and chargino searches (see 3.1) was also used in this case. The best efficiency is obtained when the dominant coupling is λ_{122} ; in this case, the same analysis used for the neutralino and chargino decay study (see Section 3.1.1) is applied, giving an efficiency of 34% for $m_{\tilde{t}} = 70 \text{ GeV}/c^2$ and $m_{\tilde{\chi}_0} = 50 \text{ GeV}/c^2$. A more detailed study has been performed to determine efficiencies in case of a dominant λ_{133} coupling, since it leads to the most conservative limit on the stop mass. The same selection criteria as described in Section 3.1.2 are used, but since in case of stop pair production, the final state always contains two jets, a minimal multiplicity of eight charged tracks is required. The distributions of the number of identified leptons, of

the missing energy and of the product $E_{min}^j * \theta_{min}^{j_1, j_2}$ versus the number of charged tracks obtained after preselection criteria are shown on Fig. 5.

At least two identified leptons are required, and in the case of two or three identified leptons, there should be no other charged track in a 10 degree half cone around them. The final criteria based on the jet characteristics and topologies are slightly modified: first, $\log_{10}(Y_{34})$ must be greater than -2.5, and second, in case of a four jet topology, four charged jets are required and the value of $E_{min}^j \times \theta_{min}^{j_a j_b}$ must be greater than 5 GeV rad. 3 events remain after the selection procedure, with 4.9 expected from background contribution (see Table 13).

Selection efficiencies vary with the stop mass and with the mass difference between the stop and the lightest neutralino. If this mass difference is higher than 5 GeV/c², the efficiency lies between 21 and 29%. In the degenerate case (i.e the mass difference is around 5 GeV/c²), the efficiency decreases and lies between 15 and 19%. This analysis is not sensitive to mass differences below 5 GeV/c².

4 Interpretation of λ dominant searches in terms of MSSM parameters

By performing the analyses described in the previous sections at $\sqrt{s} = 183$ GeV, no excess of events was found in the data with respect to the Standard Model expectation. As a consequence, limits on the production cross section and the mass of the sparticles can be set. Similar searches performed by the other three LEP experiments have also shown no evidence for R_p violating effects [21].

4.1 Results from neutralino and chargino studies

Both direct and indirect decays of pair production of charginos and neutralinos are combined to give the exclusion contours at 95 % C.L. in the μ, M_2 plane. For each coupling, the analysis is sensitive to most of the possible decay channels of neutralinos and charginos produced in the three processes considered ($\tilde{\chi}_1^0 \tilde{\chi}_1^0, \tilde{\chi}_2^0 \tilde{\chi}_1^0, \tilde{\chi}_1^+ \tilde{\chi}_1^-$). Then, the number of expected events N_{exp} , for a given set of MSSM parameters is:

$$N_{exp} = \mathcal{L} \times \sum_{i=1}^{i=3} \epsilon_i \sigma_i$$

where ϵ_i gives the efficiency for each process, σ_i the corresponding cross section and \mathcal{L} the integrated luminosity. The maximum number of signal events N_{95} in presence of background is given by the standard formula [22]. All the points in the μ, M_2 plane which satisfy the condition $N_{exp} > N_{95}$ are excluded at 95% C.L. The exclusion contours for two values of $\tan\beta$ and m_0 are shown on Fig. 6. The light grey area shows the region excluded by the λ_{133} search and the dark grey area the region excluded by the λ_{122} search which, having a better efficiency, includes and extends the excluded region. One can consider these two searches as the most and the least sensitive cases. The other couplings have a sensitivity lying in between these two extremes. This result can be translated into a lower limit on neutralino mass as shown in the Fig. 7, which was obtained by scanning over m_0 values for each $\tan\beta$ in order to set a limit independent of the choice of m_0 . With this search, neutralinos with masses less than 27 GeV/c² are excluded at 95 % C.L. whereas the corresponding limit for charginos is 89 GeV/c².

4.2 Results from sneutrino studies

A sneutrino can decay either directly into two charged leptons, or indirectly into a neutralino and a neutrino; the decay to chargino+lepton is kinematically inaccessible for a sneutrino mass up to $\simeq 90 \text{ GeV}/c^2$.

For any given λ_{ijk} coupling, only the $\tilde{\nu}_i$ and $\tilde{\nu}_j$ can decay directly into two charged leptons and have only one possible direct decay mode. In the case of λ_{122} coupling, the final states are $\mu\mu\mu\mu$ ($\tilde{\nu}_e$ pair) or $ee\mu\mu$ ($\tilde{\nu}_\mu$ pair); in the case of λ_{133} coupling, the final states are $\tau\tau\tau\tau$ ($\tilde{\nu}_e$ pair) or $ee\tau\tau$ ($\tilde{\nu}_\tau$ pair). The 4 τ final state is also possible in the case of $\tilde{\nu}_\mu$ pair decaying with a λ_{233} coupling. The efficiencies obtained for these channels, for different values of the sneutrino mass, combined with the results of the selection on data and background, allow the derivation of a limit on the cross section as a function of the $\tilde{\nu}$ mass, shown on Fig. 8. On the same plot the MSSM cross sections of $e^+e^- \rightarrow \tilde{\nu}\tilde{\nu}$ versus the $\tilde{\nu}$ mass are reported; in the case of $\tilde{\nu}_\mu$ and $\tilde{\nu}_\tau$, the pair production cross section depends only on the $\tilde{\nu}$ mass; in case of $\tilde{\nu}_e$, it may have a dependance on the MSSM parameters since it depends on the mass of the chargino exchanged in the t -channel. When the chargino mass is greater than $400 \text{ GeV}/c^2$, $\sigma(e^+e^- \rightarrow \tilde{\nu}_e\tilde{\nu}_e) = \sigma(e^+e^- \rightarrow \tilde{\nu}_\mu\tilde{\nu}_\mu)$. The dashed upper curve on the plot is the cross section obtained with a chargino mass $\simeq 90 \text{ GeV}/c^2$. From this figure, one can see that the limit on the mass of a sneutrino decaying directly into two leptons is $63 \text{ GeV}/c^2$.

The indirect decay of the sneutrino into a neutrino and a neutralino gives the same signature as the neutralino \tilde{R}_p decay with the bonus of extra missing energy. It does not depend on the sneutrino flavour, but only on the λ_{ijk} coupling. As for the charginos/neutralinos, the most conservative limit is obtained from the λ_{133} coupling. Taking into account the efficiencies obtained for several values of sneutrino and neutralino masses, and the analysis results, an exclusion area is determined in the $m_{\tilde{\nu}}, m_{\tilde{\chi}_1^0}$ plane (Fig. 9). The largest exclusion area is obtained for $e^+e^- \rightarrow \tilde{\nu}_e\tilde{\nu}_e$, with a chargino mass close to the kinematic limit. The smallest exclusion area is obtained from $\tilde{\nu}_\mu\tilde{\nu}_\mu, \tilde{\nu}_\tau\tilde{\nu}_\tau$, and is also valid for $\tilde{\nu}_e\tilde{\nu}_e$ in case of a heavy chargino. Since the efficiencies are lower for the light neutralinos, the exclusion domain is reduced compared to that of heavier neutralinos. Taking into account the limit of the neutralino mass at $27 \text{ GeV}/c^2$, the lower bound on sneutrino mass is $62 \text{ GeV}/c^2$, in the case of indirect decay. On the same plot the limits obtained in case of direct decay are reported. The line labelled λ_{233} corresponds to $\tilde{\nu}_\mu$ pair production leading to a 4 τ final state. This limit is lower than the one obtained for the indirect decay into $\tilde{\chi}_1^0\nu$ via a λ_{133} coupling when $m_{\tilde{\chi}_1^0}$ is greater than $30 \text{ GeV}/c^2$, since in this case the final state is a mixing of $4\tau, 1e3\tau, 2e2\tau$, and the efficiency is slightly higher. According to these results, a sneutrino lower than $62 \text{ GeV}/c^2$ is excluded at 95% C.L.

4.3 Results from charged slepton studies

A slepton can decay either directly into a charged lepton and a neutrino, or indirectly into a neutralino and a charged lepton; the decay to chargino+neutrino is kinematically inaccessible for a slepton mass up to $90 \text{ GeV}/c^2$. Right handed sleptons have been studied here, because their production cross section is lower than the left handed one, therefore leading to more conservative results.

For the direct searches, the results obtained from the three analyses described in Section 3.3 are combined and limits on the production cross section as a function of slepton mass are derived at 95% C.L (Fig. 10). Considering the MSSM cross section, a lower limit on the slepton mass is set at $61 \text{ GeV}/c^2$.

For the indirect searches, the most conservative limit is obtained considering the λ_{133} coupling as stated before. With the results of the analyses described in section 3.3, an exclusion region is derived in the $m_{\tilde{t}}, m_{\tilde{\chi}_1^0}$ plane (Fig. 11). Direct topologies lead to worst limits on slepton masses as the remaining background is higher than in case of indirect ones. Therefore our present lower limit on the slepton mass is $61 \text{ GeV}/c^2$ at 95% C.L.

4.4 Results from stop studies

From the study of the stop indirect decay in charm and neutralino, with the subsequent R_p decay of the neutralino in leptons a lower limit on the stop pair production cross section was derived, according to the number of observed and expected events and to the efficiencies obtained for different stop and neutralino mass. On Fig. 12 the MSSM cross section for the stop pair production as a function of the stop mass is presented for a pure left stop (mixing angle = 0 degree), and for a stop decoupled from the Z boson (mixing angle = 56 degree); considering the worst and the best efficiencies obtained for a given stop mass, the worst and the best lower limits on the cross section can be plotted. Since efficiencies have been determined for several values of the neutralino mass, an exclusion plot can be derived in $m_{\tilde{t}}, m_{\tilde{\chi}_1^0}$ plane, as shown in Fig. 13. Using our result on the neutralino mass limit of $27 \text{ GeV}/c^2$ the lower bound on stop mass is $61 \text{ GeV}/c^2$.

Coupling	Process	Efficiency range in %	Selected events	
			Data	MC
λ_{122}	$\tilde{\chi}_1^0 \tilde{\chi}_1^0$	45–60	0	0.7 ± 0.1
	$\tilde{\chi}_2^0 \tilde{\chi}_1^0$	25–40		
	$\tilde{\chi}_1^+ \tilde{\chi}_1^-$	20–50		
λ_{133}	$\tilde{\chi}_1^0 \tilde{\chi}_1^0$	22–34	3	3.3 ± 0.3
	$\tilde{\chi}_2^0 \tilde{\chi}_1^0$	20–25		
	$\tilde{\chi}_1^+ \tilde{\chi}_1^-$	20–37		

Table 7: Neutralino and chargino analyses: efficiency ranges for pair production processes, and data and Monte-Carlo events selected for each studied coupling.

Data	MC	$\gamma\gamma$	$Z\gamma$	ZZ
0	0.73 ± 0.19	0.14 ± 0.01	0.19 ± 0.18	0.40 ± 0.06

Table 8: SM background contributions for λ_{122} sneutrino analysis.

Data	MC	$\gamma\gamma$	Ze^+e^-	W^+W^-	ZZ
1	1.81 ± 0.28	0.57 ± 0.20	0.14 ± 0.14	0.67 ± 0.11	0.42 ± 0.07

Table 9: Main SM background contributions in the sneutrino analysis, in case of λ_{133} coupling.

Coupling	Process	Characteristics	Efficiency range in %	Selected events	
				Data	MC
λ_{122}	$\tilde{\nu}_e \rightarrow \mu^+ \mu^-$	Direct decay	60–80	0	0.8 ± 0.1
	$\tilde{\nu}_\mu \rightarrow e^\pm \mu^\mp$	Direct decay	50–70		
λ_{133}	$\tilde{\nu}_e \rightarrow \tau^+ \tau^-$	Direct decay	32–37	1	1.8 ± 0.2
	$\tilde{\nu}_\tau \rightarrow e^\pm \tau^\mp$	Direct decay	41–47		
	$\tilde{\nu} \rightarrow \tilde{\chi}_1^0 \nu$	$20 < \tilde{\chi}_1^0 \text{ mass} < 30$	18–29		
		$30 < \tilde{\chi}_1^0 \text{ mass} < 40$	27–36		
	$\tilde{\chi}_1^0 \text{ mass} > 40$	35–39			

Table 10: Sneutrino analysis: efficiency ranges in the different studied cases, and data and Monte-Carlo events remaining after the applied selection. Sneutrinos were generated with masses in the range 50–90 GeV/ c^2 .

Channel	Efficiencies (%) as function of $\tilde{\tau}$ mass (GeV/ c^2)							Selected events	
	50	55	60	65	70	75	80	Data	Background
$e e + \cancel{E}$	30	32	35	33	35	41	40	0	1.3 ± 0.1
$e \tau + \cancel{E}$	19	21	22	22	22	27	29	1	2.8 ± 0.2

Table 11: Slepton direct decay: efficiencies for several values of $\tilde{\tau}$ masses and data and Monte-Carlo events remaining after the applied selection, for both channels.

Coupling	Process	$\tilde{\chi}_1^0$ mass range in GeV/c^2	Efficiency range in %	Selected events	
				Data	MC
λ_{122}	$\tilde{\mu} \rightarrow \mu \tilde{\chi}_1^0$	50-80	70-80	0	0.3 ± 0.1
λ_{133}	$\tilde{e} \rightarrow e \tilde{\chi}_1^0$	50-80	35-39	1	1.8 ± 0.3
	$\tilde{\mu} \rightarrow \mu \tilde{\chi}_1^0$	50-80	42-48		
	$\tilde{\tau} \rightarrow \tau \tilde{\chi}_1^0$	25-35	24-29		
	$\tilde{\tau} \rightarrow \tau \tilde{\chi}_1^0$	35-45	25-32		
		45-80	26-34		

Table 12: Slepton analyses: efficiency ranges in the different cases studied and data and Monte-Carlo events remaining after the applied selection. Sleptons were generated with masses in the range 50–90 GeV/c^2 .

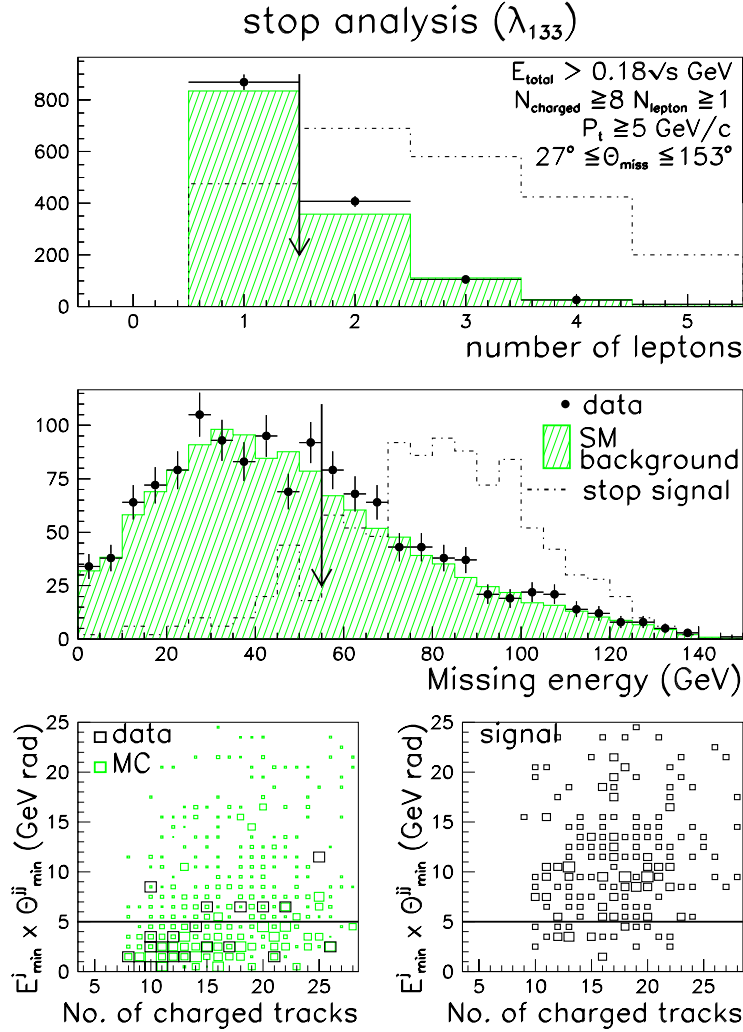


Figure 5: Stop indirect decay with the λ_{133} coupling dominant. The two upper plots show the number of leptons and the missing energy distributions for real data (black dots), expected SM background (hatched) and scaled signal (dotted line) obtained during the preselection procedure; the arrows indicate the cut values. The two lower plots show the $E_{\min}^j * \theta_{\min}^{j1, j2}$ versus the number of charged tracks for the data and the SM background (on the left) and for the signal (on the right) after the cut $N_{lepton} \geq 2$; the horizontal line illustrates the cut.

Selection criteria	Data	MC
at least one loose lepton		
$N_{charged} \geq 8$		
$E_{charged} \geq 18\% \sqrt{s}$, $E_{tot} \geq 16\% \sqrt{s}$		
missing $p_t > 5 \text{ GeV}/c$		
$27^\circ \leq \Theta_{miss} \leq 153^\circ$		
$E_{miss} > 30\% \sqrt{s}$	508	453 ± 7
$E_{max}^l \geq 5 \text{ GeV}$	347	315 ± 6
$\Theta_{lepton-track}^{min} \geq 10^\circ$ if $N_{lepton} \leq 3$	125	116 ± 2
$N_{lepton} \geq 2$	21	19.7 ± 1.3
$\log_{10}(Y_{34}) \geq -2.5$	18	17.5 ± 1.2
case of four jets :		
at least four charged jets		
$E_{min}^j * \theta_{min}^{j_1, j_2} \geq 5 \text{ GeV.rad}$		
$20^\circ \leq \theta_{jet} \leq 160^\circ$	3	4.9 ± 0.5

Table 13: Selection criteria for the stop indirect decay analysis.

Gaugino searches at $\sqrt{s} = 183$ GeV

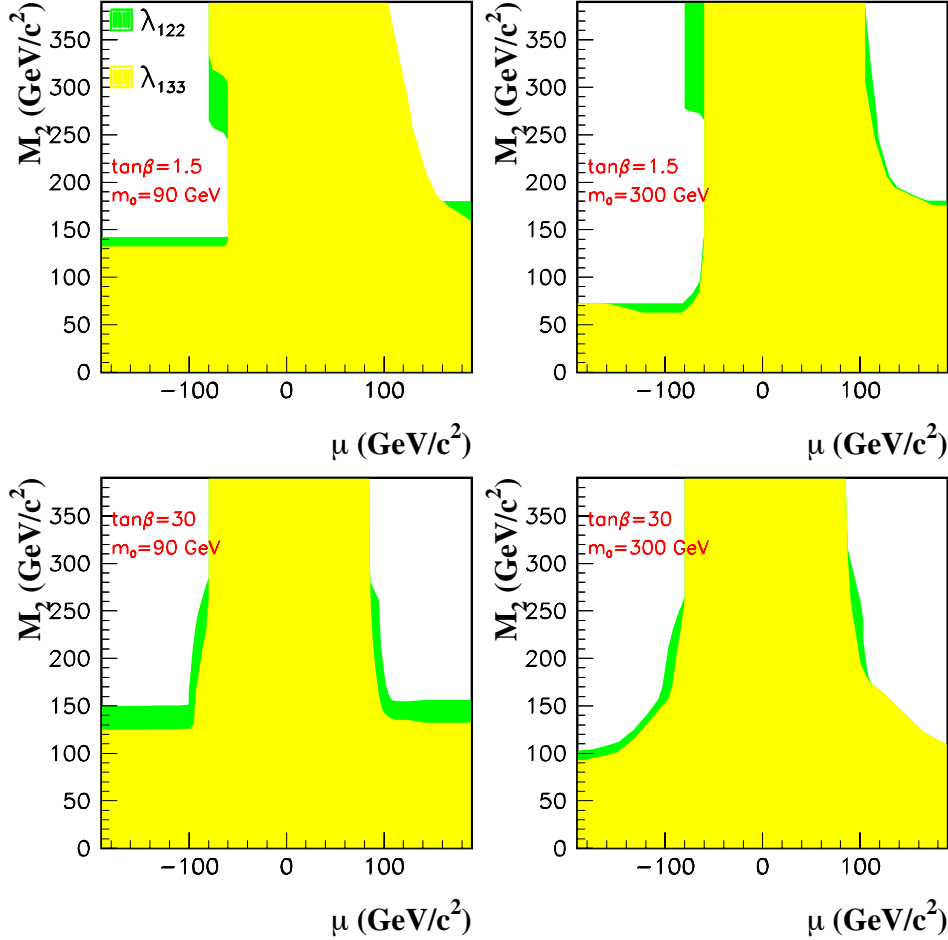


Figure 6: Neutralino and chargino searches with a dominant λ coupling: regions in μ , M_2 parameter space excluded at 95 % C.L. for two values of $\tan\beta$ and two values of m_0 . The exclusion area obtained from the λ_{133} search is shown in light grey and the corresponding area for the λ_{122} search is shown in dark grey. The second exclusion area includes the first. The data collected at $E_{CM} = 183$ GeV are used.

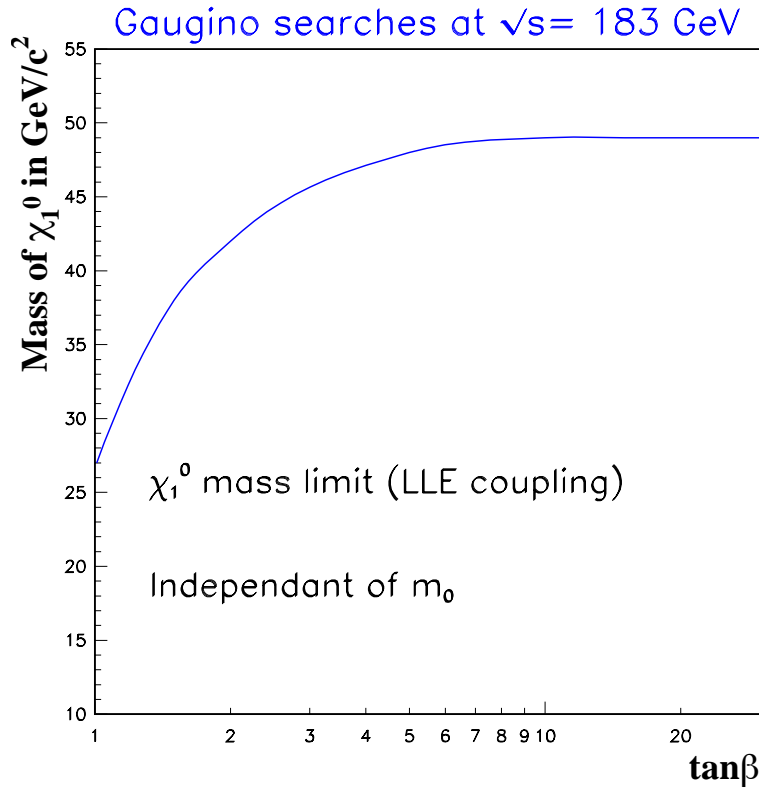


Figure 7: The lightest neutralino mass as a function of $\tan\beta$ at 95 % confidence level. This limit is independent of the choice of m_0 and the generation indices i, j, k of the λ_{ijk} coupling.

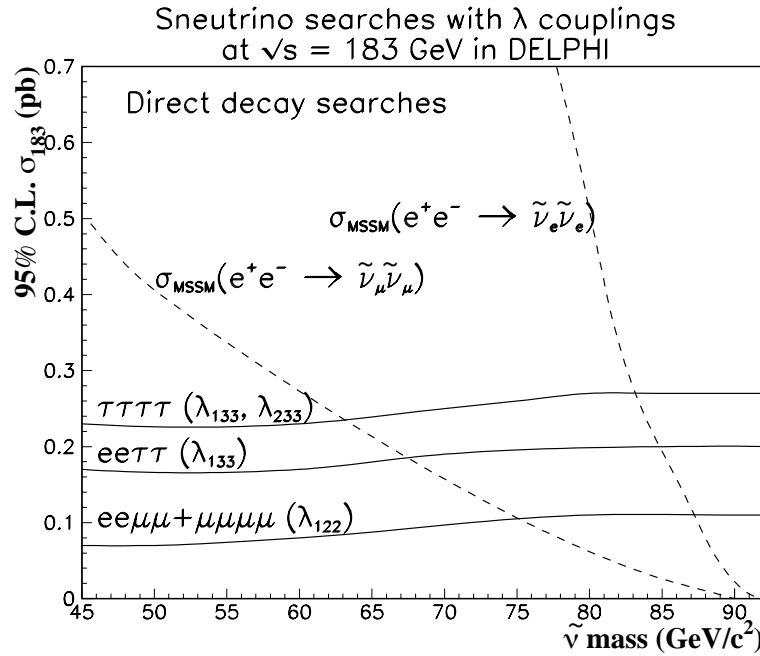


Figure 8: Sneutrino direct decay with λ coupling: the limit on the $\tilde{\nu}\tilde{\nu}$ production cross section as a function of the mass is plotted for different final states. The MSSM cross sections are reported, in order to derive a limit on the sneutrino mass in the case of direct \tilde{R}_p decay. The dashed upper curve on the plot is the $\tilde{\nu}_e\tilde{\nu}_e$ cross section obtained with a chargino mass $\simeq 90$ GeV/c^2 .

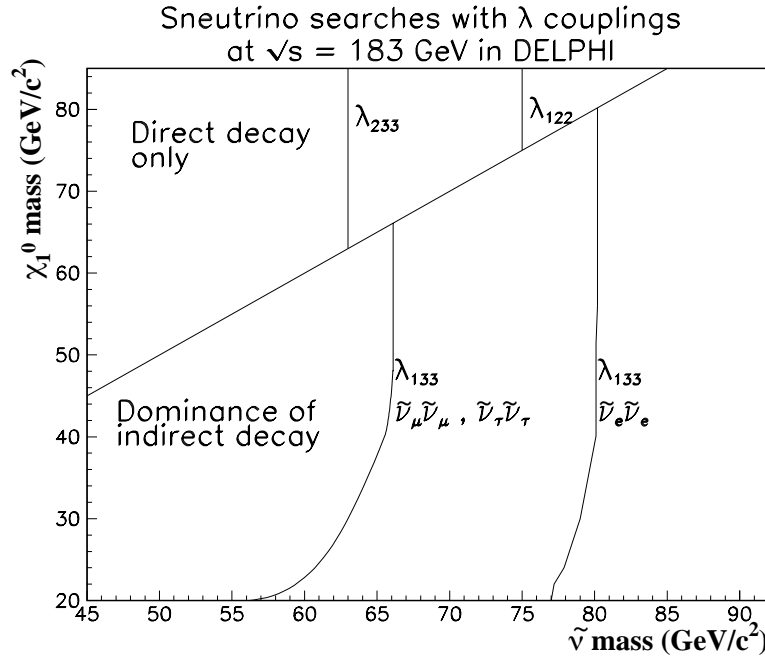


Figure 9: Sneutrino search with λ coupling: exclusion domain in $m_{\tilde{\chi}^0}$ versus $m_{\tilde{\nu}}$ for the $\tilde{\nu}$ pair production cross section; the diagonal line separates the plot into two regions: in the upper part, only the direct decay is allowed; in the lower part, the indirect decay is dominant, so the exclusion limit depends also on the neutralino mass. In both cases, only the most conservative limit has been reported, for the $\tilde{\nu}_\mu$ and $\tilde{\nu}_\tau$ production, and for the $\tilde{\nu}_e$ in case of chargino mass close to the kinematic limit.

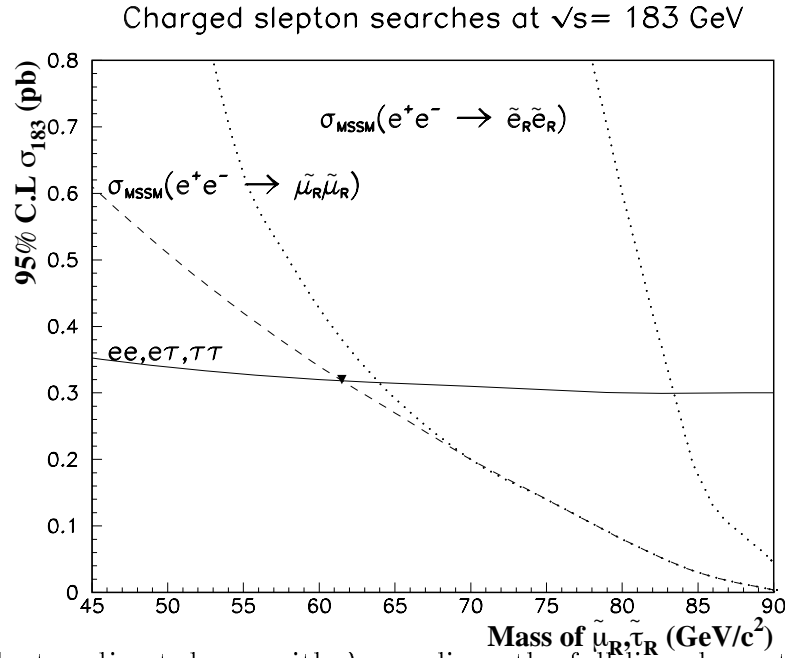


Figure 10: Slepton direct decay with λ coupling: the full line shows the limit on the $\tilde{l}\tilde{l}$ cross section as a function of the slepton mass. The dashed curve gives the MSSM cross section for $\tilde{\mu}\tilde{\mu}$, $\tilde{\tau}\tilde{\tau}$ production. The other two dotted curves show the bounds of the $\tilde{e}\tilde{e}$ cross section since it depends on neutralino mass.

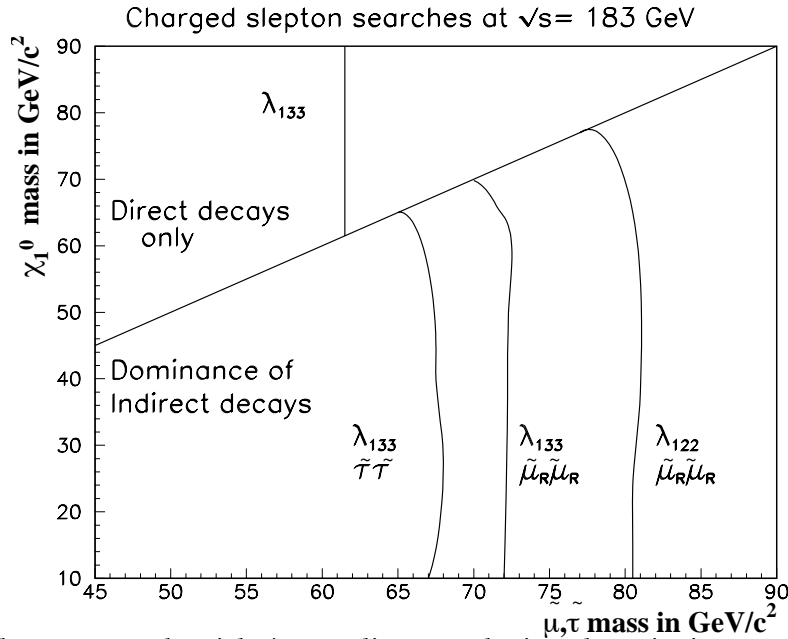


Figure 11: Slepton search with λ coupling: exclusion domain in $m_{\tilde{\chi}^0}$ versus $m_{\tilde{l}}$ for the $\tilde{l}\tilde{l}$ pair production cross section; the diagonal line separates the plot into two regions: in the upper part, only the direct decay is allowed; in the lower part, the indirect decay is dominant, so the exclusion limit depends also on the neutralino mass. The limit is given by the direct decay.

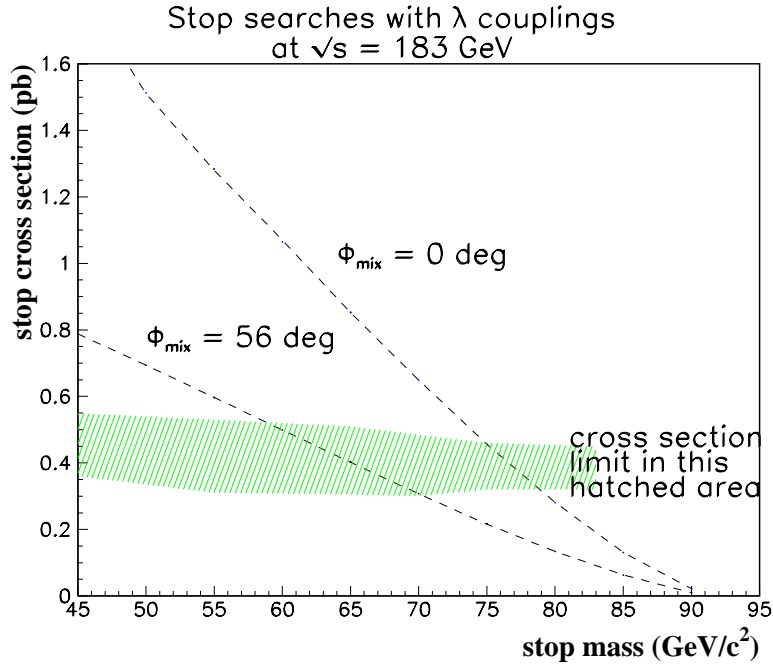


Figure 12: Stop indirect decay with λ coupling: the dotted curves give the MSSM $\tilde{t}\tilde{t}$ cross section as a function of the stop mass; the lower curve corresponds to a mixing angle of 56 degrees, the upper one to a mixing angle of 0 degree. The upper limit on the $\tilde{t}\tilde{t}$ cross section lies in the hatched area; the upper bound of this area is obtained for a mass difference between $\tilde{\chi}_1^0$ and \tilde{t} around 5 GeV/c^2 (lowest efficiency), the lower bound is determined considering the best selection efficiency for each stop mass.

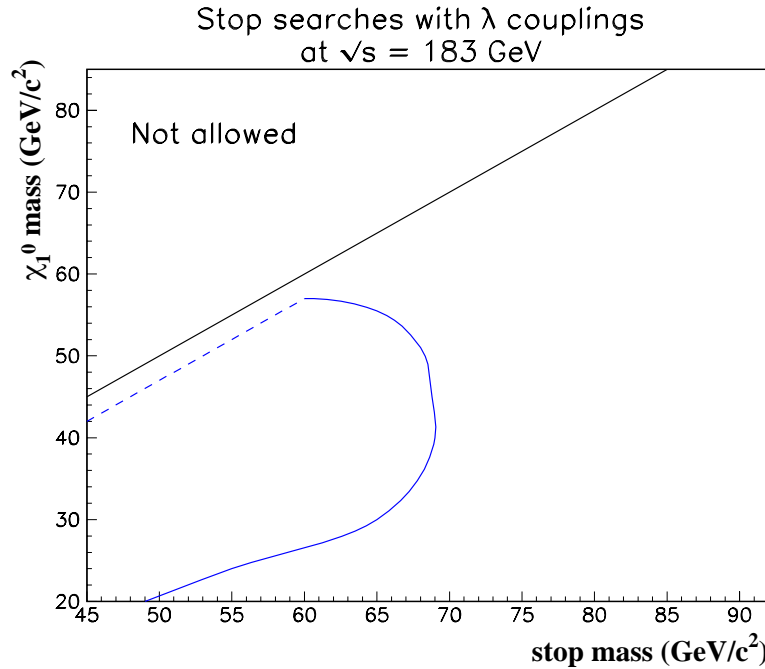


Figure 13: Stop indirect decay with λ coupling: exclusion domain in $m_{\tilde{\chi}^0}$ versus $m_{\tilde{t}}$ for the \tilde{t} pair production; the diagonal line separates the plot into two regions: in the upper part, no R_p decay of \tilde{t} is allowed; in the lower part, the indirect decay in $c\tilde{\chi}_1^0$ is allowed, so the exclusion limit depends on the neutralino mass.

5 Conclusion

Searches for \mathcal{R}_p effects in e^+e^- collisions at $\sqrt{s} = 183$ GeV have been performed with the DELPHI detector. The pair production of supersymmetric particles has been studied for the λ type of \mathcal{R}_p operators assuming that the LSP has a negligible lifetime and that the λ couplings are strong enough for the LSP to decay inside the detector. No evidence for R -parity violation has been observed so far, which allow the exclusion of a large domain of MSSM parameters. In all the cases the most conservative limit has been derived which is valid for all the generation indices i, j, k of the λ_{ijk} coupling.

From the study of the neutralino and chargino direct and indirect decays, a limit on the mass of the lightest neutralino of $27 \text{ GeV}/c^2$ has been deduced. This limit is set independently of the choice of m_0 . Furthermore a chargino with mass lighter than $89 \text{ GeV}/c^2$ at 95% C.L. has been excluded.

Studies of both direct and indirect decays of charged sleptons and sneutrinos have been performed. The most conservative mass limit of $61 \text{ GeV}/c^2$ on the charged sleptons has been obtained by the study of their direct \mathcal{R}_p decay, as opposed to the sneutrino case in which the most conservative result was obtained by the study of the indirect \mathcal{R}_p decays and led to a lower mass limit of $62 \text{ GeV}/c^2$.

Finally, studies of the indirect stop decay into a charm quark and a neutralino and the subsequent decay of the neutralino via λ couplings, led to a limit on the squark mass of $61 \text{ GeV}/c^2$.

Acknowledgements

We are greatly indebted to our technical collaborators, to the members of the CERN-SL Division for the excellent performance of the LEP collider, and to the funding agencies for their support in building and operating the DELPHI detector.

We acknowledge in particular the support of

Austrian Federal Ministry of Science and Traffics, GZ 616.364/2-III/2a/98,

FNRS-FWO, Belgium,

FINEP, CNPq, CAPES, FUJB and FAPERJ, Brazil,

Czech Ministry of Industry and Trade, GA CR 202/96/0450 and GA AVCR A1010521,

Danish Natural Research Council,

Commission of the European Communities (DG XII),

Direction des Sciences de la Matière, CEA, France,

Bundesministerium für Bildung, Wissenschaft, Forschung und Technologie, Germany,

General Secretariat for Research and Technology, Greece,

National Science Foundation (NWO) and Foundation for Research on Matter (FOM),

The Netherlands,

Norwegian Research Council,

State Committee for Scientific Research, Poland, 2P03B06015, 2P03B03311 and SPUB/P03/178/98,

JNICT-Junta Nacional de Investigação Científica e Tecnológica, Portugal,

Vedecka grantova agentura MS SR, Slovakia, Nr. 95/5195/134,

Ministry of Science and Technology of the Republic of Slovenia,

CICYT, Spain, AEN96-1661 and AEN96-1681,

The Swedish Natural Science Research Council,

Particle Physics and Astronomy Research Council, UK,

Department of Energy, USA, DE-FG02-94ER40817.

References

- [1] For reviews, see e.g. H.P. Nilles, *Phys. Rep.* **110** (1984) 1; H.E. Haber and G.L. Kane, *Phys. Rep.* **117** (1985) 75.
- [2] P. Fayet, *Phys. Lett.* **B69** (1977) 489; G. Farrar and P. Fayet, *Phys. Lett.* **B76** (1978) 575.
- [3] S. Weinberg, *Phys. Rev.* **D26** (1982) 287.
- [4] I. Hinchliffe and T. Kaeding, *Phys. Rev.* **D47** (1993) 279.
- [5] C.E. Carlson et al., *Phys. Lett.* **B357** (1995) 99.
- [6] V. Barger, G.F. Guidice and T. Han, *Phys. Rev.* **D40** (1989) 2987.
- [7] S. Dawson, *Nucl. Phys.* **B261** (1985) 297.
- [8] H. Dreiner and G.G. Ross, *Nucl. Phys.* **B365** (1991) 597.
- [9] H. Dreiner, hep-ph/9707435.
- [10] G. Bhattacharyya, hep-ph/9709395 and *Nucl. Phys.***B** (*Proc. Suppl.*) **52A** (1997) 83.
- [11] P. Abreu et al., *Nucl. Instr. Meth.* **378** (1996) 57.
- [12] T. Sjostrand, *Computer Phys. Comm.* **39** (1986) 347.
- [13] F.A. Berends, R. Kleiss and R. Pittau, *Computer Phys. Comm.* **85** (1995) 437.
- [14] F.A. Berends, P.H. Davervelt and R. Kleiss, *Computer Phys. Comm.* **40** (1986) 271,285 and 309.
- [15] S. Nova, A. Olshevski and T. Todorov, DELPHI 90-35 PROG 152.

- [16] S. Jadach and Z. Was, *Computer Phys. Comm.* **79** (1994) 503.
- [17] J.E. Campagne and R. Zitoun, *Zeit. Phys.* **C43** (1989) 469.
- [18] S. Katsanevas and P. Morawitz, hep-ph/9711417, submitted to *Comp. Phys. Comm.*
- [19] S. Catani et al., *Phys. Lett.* **B269** (1991) 432.
- [20] M. Berggren, M. Gandelman and J.H.Lopes, DELPHI 97-156 PHYS 735.
- [21] ALEPH Collaboration (R. Barate et al.) *Eur. Phys. J.* **C4** (1998) 433
.Contributions for ICHEP'98:
ALEPH Collaboration, ALEPH 98-070 CONF 98-039;
DELPHI Collaboration, DELPHI 98-138 CONF 199;
L3 Collaboration, L3 Note 229;1
OPAL Collaboration, Physics Notes 356, 359.
- [22] Particle Data Group, *Phys. Rev.* **D54** (1996) 1.